

Correlated shallow impurity bands in doped semiconductors

An-qi Lü

Department of Physics, Beijing University of Iron and Steel Technology, Beijing, China

Zhao-qing Zhang

Institute of Physics, Chinese Academy of Sciences, Beijing, China

K. A. Chao and Jia-Lin Zhu*

Department of Physics and Measurement Technology, University of Linköping, S-58183 Linköping, Sweden

(Received 12 December 1984)

The electron-correlation effect has been incorporated to the disorder model of Matsubara and Toyozawa to study the shallow impurity states in doped semiconductors. A detailed Green's-function analysis reveals the split-impurity-subband structure as a consequence of the electron correlation, in agreement with the result of computer simulations. The impurity conductivity has been investigated with an application to phosphorus-doped silicon.

I. INTRODUCTION

The random position of impurities in doped semiconductors gives rise to the disordered nature of these systems which exhibit the metal-insulator transition when the impurity concentration N is varied across a critical concentration N_c . However, both experimental and theoretical analyses suggest strongly that not only the disorder but also the electron correlation is responsible for the metal-insulator transition. Evidently, the interplay between the electron-correlation and the disorder effects makes doped semiconductors the most-studied disordered system in recent years.¹

Theoretical formulations for the electronic properties of doped semiconductors have developed along two complementary lines. Starting from the heavily doped high-concentration regime, electrons are assumed to occupy the conduction-band states of the host semiconductor and are scattered by the randomly positioned impurity potentials. The major issue is that approaching the critical concentration N_c , multiple scatterings become dominating and eventually trap the electrons in localized states. Only recently have Serre and Ghazali² succeeded in using the Klauder multiscattering approximation to demonstrate the formation of the conduction-band tail which splits off from the main band, giving the identity of an impurity band as the impurity concentration decreases.

On the other hand, one can start with very low concentration, where the intrainpurity Coulomb repulsion enhances the Anderson localization. As impurity bands emerge with increasing impurity concentration, the intrainpurity correlation splits each impurity band into two subbands. Except for the recent work of Figueira *et al.*,³ almost all the existing calculations concentrate on the lowest-lying impurity band. In this case many authors have incorporated the s -band Hubbard model⁴ to the Matsubara-Toyozawa⁵ configuration-average scheme to investigate the combined electron-correlation and disorder effects in doped semiconductors.⁶⁻⁹

The s -band Hubbard model has been extensively studied for its simplicity in dealing with the short-range correlation, which drives the metal-insulator transition. Because of this historical development, the experimental confirmation of the existence of an upper Hubbard subband in lightly doped semiconductors^{10,11} stimulated much interest in the detailed structure of impurity states in the regime of low and intermediate doping concentrations. A simple but instructive picture of the formation of split impurity subbands can be described as follows. The impurity orbital of a nondegenerate semiconductor (for example, CdS) can be well approximated by a hydrogenic $1s$ function with an effective Bohr radius $\phi_\sigma(\mathbf{r}-\mathbf{R})$, where σ is the spin index and \mathbf{R} is the position of the impurity. Let E_1 and E_2 be the ionization energies of an *isolated* impurity when it is neutral (D^0) and negatively charged (D^-), respectively. As the impurity concentration N is increased, the overlap matrix element $\langle \phi_\sigma(\mathbf{r}-\mathbf{R}_i) | \phi_\sigma(\mathbf{r}-\mathbf{R}_j) \rangle$ is no longer negligible if $|\mathbf{R}_i - \mathbf{R}_j|$ is not very large. Then, the two energy levels E_1 and E_2 spread into split impurity subbands separated by a gap.

The random spatial distribution of impurities complicates the structure of the impurity band. Before the impurity band is fully developed with increasing impurity concentration, impurity clusters of various sizes will form first. Furthermore, depending on the geometrical structure and local environment, impurity clusters can be charged (both positively and negatively) to different degrees. An enormous amount of experimental efforts has been devoted to the clarification of the nature of these *charged* cluster states.¹²⁻²⁰ However, theoretical works on charged cluster states are mostly for a single D^- center^{21,22} or a small cluster of impurities.^{23,24} We should point out that there exists a rich variety of important papers regarding the physical properties of impurity clusters which are not necessarily charged. Here we particularly mention the D^- state because of its relevance to the present work.

A complete description of shallow impurity electrons in doped semiconductors, with impurity concentration varying from the insulating to the metallic regimes, thus requires a full treatment of three bands: two split impurity subbands and one host conduction band. So far this remains an impossible task. Existing sophisticated theoretical analyses consider either only the split impurity subbands, or the host conduction band plus an uncorrelated impurity band. By uncorrelated impurity band we mean no distinction between the D^0 and the D^- states. For example, the density-functional approach of Ghazali and Leroux-Hugon²⁵ belongs to this category.

In this paper we will perform a detailed analysis on the formation of split impurity subbands with emphasis on the effect of electron correlation. Not only is the intra-impurity Coulomb energy retained—the correlation effect on the electron hopping is also taken into account. In order to perform such calculation, we have used Chandrasekhar's correlated two-particle wave function.²⁶ The random feature of the impurity distribution is treated within the framework of the Matsubara-Toyozawa scheme.⁵ As we will see in the later sections, the resulting coupled integral equations are so complicated that in this first attempt it is worthwhile to obtain a transparent physical picture with a fewer number of bands. Hence, the host conduction band is ignored and only the $1s$ impurity band will be considered. In this scope the result of large-scale computer simulation is available for comparison.^{27,28}

At the end it becomes obvious that the present two-band approach can be generalized without difficulty to include both the host conduction band and the higher-lying excited impurity bands, provided sufficient effort is devoted to the numerical calculation.

II. CORRELATED SPLIT-BAND MODEL

We consider N randomly positioned shallow-level impurities in a unit volume of nondegenerate semiconductor (N is then the impurity concentration) with an isotropic effective mass. Though the multivalley structure can be treated similarly, we prefer to work first with this simpler version in order to keep the mathematical analysis tractable. The host semiconductor is then identified via a characteristic background dielectric constant, and we will come back to this point later. At each impurity a hydrogenic $1s$ orbital is attached. If only the short-range intra-impurity Coulomb interaction is retained, the impurity system is conventionally described by a random-site s -band Hubbard Hamiltonian

$$\bar{H} = \sum_{i,j,\sigma} t_{ij} a_{i\sigma}^\dagger a_{j\sigma} + \frac{1}{2} U \sum_{i,\sigma} n_{i\sigma} n_{i-\sigma}, \quad (1)$$

where the subscripts i and j label the impurity positions. Because of the random distribution, the transfer integrals t_{ij} 's are also random.

Let us rewrite the Hamiltonian as

$$\begin{aligned} \bar{H} = \sum_{i,j,\sigma} [& t_{ij}(1-n_{i-\sigma})a_{i\sigma}^\dagger a_{j\sigma}(1-n_{j-\sigma}) + t_{ij}(1-n_{i-\sigma})a_{i\sigma}^\dagger a_{j\sigma}n_{i-\sigma} \\ & + t_{ij}n_{i-\sigma}a_{i\sigma}^\dagger a_{j\sigma}(1-n_{i-\sigma}) + t_{ij}n_{i-\sigma}a_{i\sigma}^\dagger a_{j\sigma}n_{j-\sigma}] + \frac{1}{2} U \sum_{i,\sigma} n_{i\sigma} n_{i-\sigma}. \end{aligned} \quad (2)$$

To clarify the purpose of this rewriting, we define the correlated operators

$$\begin{aligned} b_{i\sigma}^\dagger &= (1-n_{i-\sigma})a_{i\sigma}^\dagger, \\ b_{i\sigma} &= a_{i\sigma}(1-n_{i-\sigma}), \\ c_{i\sigma}^\dagger &= n_{i-\sigma}a_{i\sigma}^\dagger, \\ c_{i\sigma} &= a_{i\sigma}n_{i-\sigma}, \end{aligned} \quad (3)$$

and we rewrite the Hamiltonian once again as

$$\begin{aligned} \bar{H} = \sum_{i,j,\sigma} [& t_{ij}b_{i\sigma}^\dagger b_{j\sigma} + t_{ij}b_{i\sigma}^\dagger c_{j\sigma} + t_{ij}c_{i\sigma}^\dagger b_{j\sigma} \\ & + (t_{ij} + \frac{1}{2} U \delta_{ij})c_{i\sigma}^\dagger c_{j\sigma}]. \end{aligned} \quad (4)$$

The four terms $b_{i\sigma}^\dagger b_{j\sigma}$, $b_{i\sigma}^\dagger c_{j\sigma}$, $c_{i\sigma}^\dagger b_{j\sigma}$, and $c_{i\sigma}^\dagger c_{j\sigma}$ represent electron transfers with four different local environments. When a σ -spin electron hops from the impurity j to the impurity i , the initial j th impurity may be either singly or doubly occupied, while the final i th impurity may be either empty or singly occupied by a ($-\sigma$)-spin electron. Therefore, we have $b_{i\sigma}^\dagger b_{j\sigma}$ from the singly occupied j th to the empty i th impurity, $b_{i\sigma}^\dagger c_{j\sigma}$ from the doubly occupied j th to the empty i th impurity, $c_{i\sigma}^\dagger b_{j\sigma}$ from the singly occupied j th to the singly occupied i th impurity, and $c_{i\sigma}^\dagger c_{j\sigma}$

from the doubly occupied j th to the singly occupied i th impurity. Certainly, the matrix elements corresponding to these physical processes are different. Since later we will use real wave functions to calculate these matrix elements, they are real and so we have the final form of our model Hamiltonian:

$$\begin{aligned} H = E_1 \sum_{i,\sigma} b_{i\sigma}^\dagger b_{i\sigma} + E_2 \sum_{i,\sigma} c_{i\sigma}^\dagger c_{i\sigma} + \sum'_{i,j,\sigma} t(1)_{ij} b_{i\sigma}^\dagger b_{j\sigma} \\ + \sum'_{i,j,\sigma} t(2)_{ij} (b_{i\sigma}^\dagger c_{j\sigma} + c_{i\sigma}^\dagger b_{j\sigma}) + \sum'_{i,j,\sigma} t(3)_{ij} c_{i\sigma}^\dagger c_{j\sigma}, \end{aligned} \quad (5)$$

where $E_1 = t_{ii}$, $E_2 = t_{ii} + U/2$, and the primed sums exclude terms with $i = j$. This correlated split-band model Hamiltonian has a clear interpretation. The terms E_1 and $t(1)_{ij}$, if alone, form the lower impurity subband. The terms E_2 and $t(3)_{ij}$, if alone, form the upper impurity subband. These two subbands are in fact not alone, and so are coupled by the term $t(2)_{ij}$.

A full many-body calculation of the matrix elements E_1 , E_2 , and $t(\nu)_{ij}$ is certainly impossible. An approximate calculation scheme is the generalization of the tight-binding method which is commonly used to treat narrow energy bands. Such an approximation is reasonable if the impurity concentration is not too high. In fact, this is the concentration regime where the short-range intra-impurity correlation dominates and so our model

Hamiltonian is justified. In the framework of the generalized tight-binding approximation, the whole impurity system is divided into two parts when one calculates the matrix elements. Let us first consider E_1 and E_2 . In this case we only solve the problem of a single impurity embedded in the effective field of the remaining $N-1$ impurities. Even if we assume a nondegenerate single-valley semiconductor and simplify the screening of valence electrons to a static dielectric constant κ , the self-consistent treatment of the polarization within the impurity system is still a difficult problem. In the tight-binding approximation this difficulty is avoided with a calculation at the extremely low impurity concentration where only the valence electrons contribute a dielectric constant κ . In other words, E_1 and E_2 are derived from an isolated hydrogenic-type impurity in D^0 and in D^- configurations, respectively. Again, because the single-valley structure is assumed, we will not consider higher-charged configurations which have been studied recently by Wu and Falicov.²⁹

We will adopt the effective hartree and the effective Bohr radius as the units of energy and length, respectively. For specific doped semiconductors the effective hartree and so the effective Bohr radius can be determined empirically. Thus, we have $E_1 = -0.5$ and the corresponding eigenstate $\phi_\sigma(\mathbf{r}-\mathbf{R}) = (1/\sqrt{\pi})\exp(-|\mathbf{r}-\mathbf{R}|)$. To calculate E_2 we should notice that $2E_2$ is the total energy of an isolated negatively-charged impurity. The two-electron wave function $\psi(\mathbf{r}_1, \mathbf{r}_2; \mathbf{R})$ is highly correlated. There exists in the literature complicated forms of $\psi(\mathbf{r}_1, \mathbf{r}_2; \mathbf{R})$; for example, the 20-term expansion of Petelenz and Smith.³⁰ Yet for the hydrogenic-type impurity considered here, the most accurate and convenient D^-

wave function is the one constructed by Chandrasekhar²⁶:

$$\begin{aligned} \psi(\mathbf{r}_1; \mathbf{r}_2; \mathbf{R}) = & \eta [\exp(-\alpha |\mathbf{r}_1 - \mathbf{R}| - \beta |\mathbf{r}_2 - \mathbf{R}|) \\ & + \exp(-\alpha |\mathbf{r}_2 - \mathbf{R}| - \beta |\mathbf{r}_1 - \mathbf{R}|)] \\ & \times [1 - \gamma (|\mathbf{r}_1 - \mathbf{r}_2|)], \end{aligned} \quad (6)$$

where $\alpha = 1.07478$, $\beta = 0.47758$, $\gamma = 0.31214$, and η is the normalization constant. The Chandrasekhar wave function yields a binding energy $E_2^* = E_1 - 2E_2 = 0.0259$ as compared to the measured value 0.0275 when applied to a free H^- ion. The charge density at the nucleus given by (6) for a free H^- ion is in error by only 2% relative to Pekeris's calculation.³¹ Besides being accurate and relatively simple, another main reason for using the Chandrasekhar wave function is that the same wave function has been used in the computer simulation^{27,28} and so we can compare our analytical result to the numerical one. The energy E_2 is thus determined as -0.26295 .

Similarly, in the tight-binding approximation we consider only the (i, j) -impurity pair to calculate the matrix elements $t(\nu)_{ij}$. For $t(1)_{ij}$ there is only one electron in this small cluster of two impurities with the initial and the final electronic wave functions $\phi_\sigma(\mathbf{r}-\mathbf{R}_j)$ and $\phi_\sigma(\mathbf{r}-\mathbf{R}_i)$, respectively. For $t(3)_{ij}$ there are three electrons and the initial and the final wave functions are, respectively, $\phi_\sigma(\mathbf{r}_1-\mathbf{R}_i)\psi(\mathbf{r}_2, \mathbf{r}_3; \mathbf{R}_j)$ and $\psi(\mathbf{r}_1, \mathbf{r}_2; \mathbf{R}_i)\phi_\sigma(\mathbf{r}_3-\mathbf{R}_j)$. Therefore, if we let $V_{\text{ion}}(r_{\mu i}) = -e^2/\kappa |\mathbf{r}_\mu - \mathbf{R}_i|$ and $V_{\text{el}}(r_{\mu\nu}) = e^2/\kappa |\mathbf{r}_\mu - \mathbf{r}_\nu|$, then with the assumption that wave functions localized on different impurities are orthogonal to each other, the tight-binding matrix elements are

$$\begin{aligned} t(1)_{ij} = & \left\langle \phi_\sigma(\mathbf{r}_1 - \mathbf{R}_i) \left| \frac{1}{2m} p_1^2 + V_{\text{ion}}(r_{1i}) + V_{\text{ion}}(r_{1j}) \right| \phi_\sigma(\mathbf{r}_1 - \mathbf{R}_j) \right\rangle \\ = & \langle \phi_\sigma(\mathbf{r}_1 - \mathbf{R}_i) | V_{\text{ion}}(r_{1i}) | \phi_\sigma(\mathbf{r}_1 - \mathbf{R}_j) \rangle, \end{aligned} \quad (7)$$

$$\begin{aligned} t(3)_{ij} = & \left\langle \psi(\mathbf{r}_1, \mathbf{r}_2; \mathbf{R}_i) \phi_\sigma(\mathbf{r}_3 - \mathbf{R}_j) \left| \sum_{\mu=1}^3 \left[\frac{1}{2m} p_\mu^2 + V_{\text{ion}}(r_{\mu i}) + V_{\text{ion}}(r_{\mu j}) \right] + V_{\text{el}}(r_{12}) \right. \right. \\ & \left. \left. + V_{\text{el}}(r_{23}) + V_{\text{el}}(r_{31}) \right| \phi_\sigma(\mathbf{r}_1 - \mathbf{R}_i) \psi(\mathbf{r}_2, \mathbf{r}_3; \mathbf{R}_j) \right\rangle \\ = & \langle \psi(\mathbf{r}_1, \mathbf{r}_2; \mathbf{R}_i) \phi_\sigma(\mathbf{r}_3 - \mathbf{R}_j) | V_{\text{ion}}(r_{1j}) + V_{\text{ion}}(r_{2i}) + V_{\text{ion}}(r_{3i}) + V_{\text{el}}(r_{12}) + V_{\text{el}}(r_{13}) | \phi_\sigma(\mathbf{r}_1 - \mathbf{R}_i) \psi(\mathbf{r}_2, \mathbf{r}_3; \mathbf{R}_j) \rangle. \end{aligned} \quad (8)$$

It is important to remind ourselves that the Chandrasekhar wave function is a variational trial function but not the exact eigenfunction of a D^- impurity. Since the real matrix elements for the two processes $b_{i\sigma}^\dagger c_{j\sigma}$ and $c_{i\sigma}^\dagger b_{j\sigma}$ must be the same, $t(2)_{ij}$ is calculated as

$$\begin{aligned} t(2)_{ij} = & \frac{1}{2} \left\langle \phi_\sigma(\mathbf{r}_1 - \mathbf{R}_i) \phi_{-\sigma}(\mathbf{r}_2 - \mathbf{R}_j) \left| \sum_{\mu=1}^2 \left[\frac{1}{2m} p_\mu^2 + V_{\text{ion}}(r_{\mu i}) + V_{\text{ion}}(r_{\mu j}) \right] + V_{\text{el}}(r_{12}) \right| \psi(\mathbf{r}_1, \mathbf{r}_2; \mathbf{R}_j) \right\rangle \\ & + \frac{1}{2} \left\langle \psi(\mathbf{r}_1, \mathbf{r}_2; \mathbf{R}_i) \left| \sum_{\mu=1}^2 \left[\frac{1}{2m} p_\mu^2 + V_{\text{ion}}(r_{\mu i}) + V_{\text{ion}}(r_{\mu j}) \right] + V_{\text{el}}(r_{12}) \right| \phi_\sigma(\mathbf{r}_1 - \mathbf{R}_i) \phi_{-\sigma}(\mathbf{r}_2 - \mathbf{R}_j) \right\rangle \\ = & \langle \phi_\sigma(\mathbf{r}_1 - \mathbf{R}_i) \phi_{-\sigma}(\mathbf{r}_2 - \mathbf{R}_j) | \frac{1}{2} [V_{\text{ion}}(r_{1i}) + V_{\text{ion}}(r_{1j}) + V_{\text{el}}(r_{12}) + V_{\text{ion}}(r_{2i})] | \psi(\mathbf{r}_1, \mathbf{r}_2; \mathbf{R}_j) \rangle. \end{aligned} \quad (9)$$

To calculate the matrix elements $t(\nu)_{ij}$ we have assumed that wave functions (both ϕ_σ and ψ) localized on different impurities are orthogonal. This assumption ensures the anticommutation relations among the operators $a_{i\sigma}^\dagger$ and $a_{i\sigma}$. However, when these wave functions were used in the computation simulation,^{27,28} there was no such assumption and the overlaps between these wave functions were explicitly taken into account. We will see later that this is the main source of discrepancy between our analytical result and that derived from the computer simulation.

To arrive at the model Hamiltonian (5) the electron-correlation effect has been used in both the matrix elements and the creation and annihilation operators. Therefore, E_2 cannot be viewed as the energy of a single electron. The correct interpretation is that $2E_2$ is the total energy of two antiparallel spin electrons when they occupy the same impurity orbital. We can decompose $2E_2$ as the sum of E_1 for the first electron with σ spin (when the impurity orbital is single occupied) and $E_1 + U$ for the second electron with $-\sigma$ spin (when the second electron is added to the singly occupied impurity orbital). Then, it is clear that the upper split impurity subband is centered around $\epsilon_2 \equiv E_1 + U$ but not around E_2 . From the above calculation we easily obtain $\epsilon_2 = -0.0259$, i.e., $|\epsilon_2|$ is the binding energy of an isolated D^- impurity.

III. GREEN'S-FUNCTION ANALYSIS

Since the positions of the impurities are random and the final result requires the configuration average, we will

first start with a fixed spatial configuration of the impurities and consider the 2×2 Green's-function matrix $\underline{G}^\sigma(i,j)$ for a given spin σ and a pair of impurities (i,j)

$$\underline{G}^\sigma(i,j) = \begin{bmatrix} G_{bb}^\sigma(i,j) & G_{bc}^\sigma(i,j) \\ G_{cb}^\sigma(i,j) & G_{cc}^\sigma(i,j) \end{bmatrix}, \quad (10)$$

where

$$G_{bb}^\sigma(i,j) = \langle\langle b_{i\sigma}(t); b_{j\sigma}^\dagger(0) \rangle\rangle, \quad (11a)$$

$$G_{bc}^\sigma(i,j) = \langle\langle b_{i\sigma}(t); c_{j\sigma}^\dagger(0) \rangle\rangle, \quad (11b)$$

$$G_{cb}^\sigma(i,j) = \langle\langle c_{i\sigma}(t); b_{j\sigma}^\dagger(0) \rangle\rangle, \quad (11c)$$

$$G_{cc}^\sigma(i,j) = \langle\langle c_{i\sigma}(t); c_{j\sigma}^\dagger(0) \rangle\rangle. \quad (11d)$$

The Fourier transforms of these Green's functions

$$G_{AB}^\sigma(i,j;E) \equiv \langle\langle A; B \rangle\rangle_E = \int_{-\infty}^{\infty} \langle\langle A(t); B(0) \rangle\rangle \exp(iEt/\hbar) dt \quad (12)$$

satisfy the equation of motion

$$E \langle\langle A; B \rangle\rangle_E = \langle [A, B]_+ \rangle + \langle\langle [A, H]_-; B \rangle\rangle_E, \quad (13)$$

where $[A, B]_+$ and $[A, B]_-$ are, respectively, the anticommutator and commutator. In calculating the equation of motion one should be aware of the fact that although $a_{i\sigma}^\dagger$ and $a_{i\sigma}$ are fermion operators, the operators $b_{i\sigma}^\dagger$, $b_{i\sigma}$, $c_{i\sigma}^\dagger$, and $c_{i\sigma}$ do not satisfy the anticommutation relation. We then obtain the following equations from Eq. (13):

$$G_{bb}^\sigma(i,j;E) = \frac{1}{E - E_1} \left[(1 - n_{-\sigma}) \delta_{ij} + \sum_{k(k \neq i)} [t(1)_{ik} \langle\langle (1 - n_{i-\sigma}) b_{k\sigma}; b_{j\sigma}^\dagger \rangle\rangle_E + t(2)_{ik} \langle\langle (1 - n_{i-\sigma}) c_{k\sigma}; b_{j\sigma}^\dagger \rangle\rangle_E] \right], \quad (14a)$$

$$G_{bc}^\sigma(i,j;E) = \frac{1}{E - E_1} \sum_{k(k \neq i)} [t(1)_{ik} \langle\langle (1 - n_{i-\sigma}) b_{k\sigma}; c_{j\sigma}^\dagger \rangle\rangle_E + t(2)_{ik} \langle\langle (1 - n_{i-\sigma}) c_{k\sigma}; c_{j\sigma}^\dagger \rangle\rangle_E], \quad (14b)$$

$$G_{cb}^\sigma(i,j;E) = \frac{1}{E - \epsilon_2} \sum_{k(k \neq i)} [t(2)_{ik} \langle\langle n_{i-\sigma} b_{k\sigma}; b_{j\sigma}^\dagger \rangle\rangle_E + t(3)_{ik} \langle\langle n_{i-\sigma} c_{k\sigma}; b_{j\sigma}^\dagger \rangle\rangle_E], \quad (14c)$$

$$G_{cc}^\sigma(i,j;E) = \frac{1}{E - \epsilon_2} \left[n_{-\sigma} \delta_{ij} + \sum_{k(k \neq i)} \{ t(2)_{ik} \langle\langle n_{i-\sigma} b_{k\sigma}; c_{j\sigma}^\dagger \rangle\rangle_E + t(3)_{ik} \langle\langle n_{i-\sigma} c_{k\sigma}; c_{j\sigma}^\dagger \rangle\rangle_E \} \right], \quad (14d)$$

where $n_\sigma = \langle n_{i\sigma} \rangle$ is the mean density of the σ -spin electrons. To arrive at the above four equations, we have used what we call the *static approximation*. When a σ -spin electron hops from the j th impurity to the i th impurity, there is possibility that a $-\sigma$ -spin electron may move into or out of either the i th or the j th, or both the i th and the j th impurities. In the static approximation, such double-hopping process of a pair of antiparallel-spin electrons taking place at a single impurity is neglected. The probability for double-hopping processes to occur is small if the impurity concentration is low. Hence, the static approximation is reasonable for the impurity system in the insulating regime.

To continue our analysis, we need to know the Green's functions on the right-hand side of Eqs. (14a)–(14d). If we apply the static approximation to the equations of motion of these higher order Green's functions, after a lengthy algebraic manipulation the results can be summarized as follows.

(a) For $i = j$, we have

$$G_{bb}^\sigma(i,i;E) = \frac{1}{E - E_1} \left[(1 - n_{-\sigma}) + \sum_{k(k \neq i)} [t(1)_{ik} G_{bb}^\sigma(k,i;E) + t(2)_{ik} G_{cb}^\sigma(k,i;E)] \right], \quad (15a)$$

$$G_{bc}^\sigma(i,i;E) = G_{cb}^\sigma(i,i;E) = 0, \quad (15b)$$

$$G_{cc}^\sigma(i,i;E) = \frac{1}{E - \epsilon_2} \left[n_{-\sigma} + \sum_{k(k \neq i)} [t(2)_{ik} G_{bc}^\sigma(k,i;E) + t(3)_{ik} G_{cc}^\sigma(k,i;E)] \right]. \quad (15c)$$

(b) For $i \neq j$ the higher Green's functions on the right-hand side of Eqs. (14a)–(14d) will be given separately for $k = j$ and for $k \neq j$. If $k = j$ we have

$$\langle\langle (1-n_{i-\sigma})b_{j\sigma}; b_{j\sigma}^\dagger \rangle\rangle_E = \frac{1}{E-E_1} \left[(1-n_{i-\sigma})^2 + \sum_{p(p \neq j)} [t(1)_{jp} \langle\langle (1-n_{i-\sigma})b_{p\sigma}; b_{j\sigma}^\dagger \rangle\rangle_E + t(2)_{jp} \langle\langle (1-n_{i-\sigma})c_{p\sigma}; b_{j\sigma}^\dagger \rangle\rangle_E] \right], \quad (16a)$$

$$\langle\langle (1-n_{i-\sigma})c_{j\sigma}; b_{j\sigma}^\dagger \rangle\rangle_E = 0, \quad (16b)$$

$$\langle\langle (1-n_{i-\sigma})b_{j\sigma}; c_{j\sigma}^\dagger \rangle\rangle_E = 0, \quad (17a)$$

$$\langle\langle (1-n_{i-\sigma})c_{j\sigma}; c_{j\sigma}^\dagger \rangle\rangle_E = \frac{1}{E-\epsilon_2} \left[(1-n_{i-\sigma})n_{-\sigma} + \sum_{p(p \neq j)} [t(2)_{jp} \langle\langle (1-n_{i-\sigma})b_{p\sigma}; c_{j\sigma}^\dagger \rangle\rangle_E + t(3)_{jp} \langle\langle (1-n_{i-\sigma})c_{p\sigma}; c_{j\sigma}^\dagger \rangle\rangle_E] \right], \quad (17b)$$

and the other four Green's functions $\langle\langle n_{i-\sigma}b_{j\sigma}; b_{j\sigma}^\dagger \rangle\rangle_E$, $\langle\langle n_{i-\sigma}c_{j\sigma}; b_{j\sigma}^\dagger \rangle\rangle_E$, $\langle\langle n_{i-\sigma}b_{j\sigma}; c_{j\sigma}^\dagger \rangle\rangle_E$, and $\langle\langle n_{i-\sigma}c_{j\sigma}; c_{j\sigma}^\dagger \rangle\rangle_E$ can be easily derived from Eqs. (15a)–(17b). To obtain these results, we have approximated $\langle n_{i\sigma}n_{j\sigma'} \rangle = n_{\sigma}n_{\sigma'}$ for $i \neq j$. On the other hand if $k \neq j$, the expressions are more complicated as

$$\begin{aligned} \langle\langle (1-n_{i-\sigma})b_{k\sigma}; b_{j\sigma}^\dagger \rangle\rangle_E &= \frac{1}{E-E_1} \sum_{p(p \neq k)} [t(1)_{kp} \langle\langle (1-n_{i-\sigma})(1-n_{k-\sigma})b_{p\sigma}; b_{j\sigma}^\dagger \rangle\rangle_E \\ &\quad + t(2)_{kp} \langle\langle (1-n_{i-\sigma})(1-n_{k-\sigma})c_{p\sigma}; b_{j\sigma}^\dagger \rangle\rangle_E], \end{aligned} \quad (18a)$$

$$\langle\langle (1-n_{i-\sigma})c_{k\sigma}; b_{j\sigma}^\dagger \rangle\rangle_E = \frac{1}{E-\epsilon_2} \sum_{p(p \neq k)} [t(2)_{kp} \langle\langle (1-n_{i-\sigma})n_{k-\sigma}b_{p\sigma}; b_{j\sigma}^\dagger \rangle\rangle_E + t(3)_{kp} \langle\langle (1-n_{i-\sigma})n_{k-\sigma}c_{p\sigma}; b_{j\sigma}^\dagger \rangle\rangle_E], \quad (18b)$$

$$\begin{aligned} \langle\langle (1-n_{i-\sigma})b_{k\sigma}; c_{j\sigma}^\dagger \rangle\rangle_E &= \frac{1}{E-E_1} \sum_{p(p \neq k)} [t(1)_{kp} \langle\langle (1-n_{i-\sigma})(1-n_{k-\sigma})b_{p\sigma}; c_{j\sigma}^\dagger \rangle\rangle_E \\ &\quad + t(2)_{kp} \langle\langle (1-n_{i-\sigma})(1-n_{k-\sigma})c_{p\sigma}; c_{j\sigma}^\dagger \rangle\rangle_E], \end{aligned} \quad (19a)$$

$$\langle\langle (1-n_{i-\sigma})c_{k\sigma}; c_{j\sigma}^\dagger \rangle\rangle_E = \frac{1}{E-\epsilon_2} \sum_{p(p \neq k)} [t(2)_{kp} \langle\langle (1-n_{i-\sigma})n_{k-\sigma}b_{p\sigma}; c_{j\sigma}^\dagger \rangle\rangle_E + t(3)_{kp} \langle\langle (1-n_{i-\sigma})n_{k-\sigma}c_{p\sigma}; c_{j\sigma}^\dagger \rangle\rangle_E], \quad (19b)$$

and by combining Eqs. (14a)–(14d) and Eqs. (18a)–(19b), we can easily derive the other four Green's functions $\langle\langle n_{i-\sigma}b_{k\sigma}; b_{j\sigma}^\dagger \rangle\rangle_E$, $\langle\langle n_{i-\sigma}c_{k\sigma}; b_{j\sigma}^\dagger \rangle\rangle_E$, $\langle\langle n_{i-\sigma}b_{k\sigma}; c_{j\sigma}^\dagger \rangle\rangle_E$, and $\langle\langle n_{i-\sigma}c_{k\sigma}; c_{j\sigma}^\dagger \rangle\rangle_E$.

From the above hierarchy of equations of motion, i.e., Eqs. (14a)–(19b), we see that if we continue to write down the equations of motion for increasingly higher order Green's functions, only *in the static approximation* is a certain class of higher order Green's functions generated. These higher order Green's functions have the general form

$$\langle\langle (1-n_{\mu_1-\sigma})(1-n_{\mu_2-\sigma}) \cdots n_{\nu_1-\sigma}n_{\nu_2-\sigma} \cdots A; B \rangle\rangle_E,$$

where $A = b_{p\sigma}$ or $c_{p\sigma}$ for arbitrary p , and $B = b_{j\sigma}^\dagger$ or $c_{j\sigma}^\dagger$. Only after we have derived the complete hierarchy of equations of motion can we apply the following decoupling scheme to all the higher order Green's functions in the whole hierarchy:

$$\begin{aligned} \langle\langle (1-n_{\mu_1-\sigma})(1-n_{\mu_2-\sigma}) \cdots n_{\nu_1-\sigma}n_{\nu_2-\sigma} \cdots A, B \rangle\rangle_E &\simeq \langle\langle (1-n_{\mu_1-\sigma})(1-n_{\mu_2-\sigma}) \cdots n_{\nu_1-\sigma}n_{\nu_2-\sigma} \cdots \rangle\rangle \langle\langle A, B \rangle\rangle_E \\ &\simeq (1-n_{-\sigma})(1-n_{-\sigma}) \cdots n_{-\sigma}n_{-\sigma} \cdots \langle\langle A, B \rangle\rangle_E. \end{aligned} \quad (20)$$

In order to put the decoupled hierarchy of equations of motion in a compact form, let us define the matrix operators

$$\mathbf{G}_0^\sigma(E) = \begin{bmatrix} (1-n_{-\sigma})/(E-E_1) & 0 \\ 0 & n_{-\sigma}/(E-\epsilon_2) \end{bmatrix}, \quad (21)$$

$$\mathbf{g}(E) = \begin{bmatrix} 1/(E-E_1) & 0 \\ 0 & 1/(E-\epsilon_2) \end{bmatrix}, \quad (22)$$

$${}^* \mathbf{T}_{ij} = \begin{bmatrix} t(1)_{ij}\delta_{ij} & t(2)_{ij}\delta_{ij} \\ t(2)_{ij}\delta_{ij} & t(3)_{ij}\delta_{ij} \end{bmatrix}, \quad (23)$$

and the projection operator \mathcal{P} operating on any matrix with the result

$$\mathcal{P} \begin{pmatrix} A & B \\ C & D \end{pmatrix} = \begin{pmatrix} A & 0 \\ 0 & D \end{pmatrix}. \quad (24)$$

Then, the Green's-function matrices satisfy the equations

$$\begin{aligned} \underline{G}^\sigma(i,i;E) &= \underline{G}_0^\sigma(E) + \underline{g}(E) \mathcal{P} \sum_{k_1} \underline{T}_{ik_1} \underline{G}_0^\sigma(E) \underline{T}_{k_1i} \underline{G}^\sigma(i,i;E) \\ &+ \underline{g}(E) \mathcal{P} \sum_{k_1, k_2} \underline{T}_{ik_1} \underline{G}_0^\sigma(E) \underline{T}_{k_1k_2} \underline{G}_0^\sigma(E) \underline{T}_{k_2i} \underline{G}^\sigma(i,i;E) \\ &+ \underline{g}(E) \mathcal{P} \sum_{k_1, k_2, k_3} \underline{T}_{ik_1} \underline{G}_0^\sigma(E) \underline{T}_{k_1k_2} \underline{G}_0^\sigma(E) \underline{T}_{k_2k_3} \underline{G}_0^\sigma(E) \underline{T}_{k_3i} \underline{G}^\sigma(i,i;E) + \dots \end{aligned} \quad (25)$$

and

$$\begin{aligned} \underline{G}^\sigma(i,j;E) &= \underline{G}_0^\sigma(E) \underline{T}_{ij} \underline{G}^\sigma(j,j;E) + \underline{G}_0^\sigma(E) \sum_{k_1} \underline{T}_{ik_1} \underline{G}_0^\sigma(E) \underline{T}_{k_1j} \underline{G}^\sigma(j,j;E) \\ &+ \underline{G}_0^\sigma(E) \sum_{k_1, k_2} \underline{T}_{ik_1} \underline{G}_0^\sigma(E) \underline{T}_{k_1k_2} \underline{G}_0^\sigma(E) \underline{T}_{k_2j} \underline{G}^\sigma(j,j;E) \\ &+ \underline{G}_0^\sigma(E) \sum_{k_1, k_2, k_3} \underline{T}_{ik_1} \underline{G}_0^\sigma(E) \underline{T}_{k_1k_2} \underline{G}_0^\sigma(E) \underline{T}_{k_2k_3} \underline{G}_0^\sigma(E) \underline{T}_{k_3j} \underline{G}^\sigma(j,j;E) + \dots \quad \text{for } i \neq j. \end{aligned} \quad (26)$$

Up to now our analysis has been restricted to a fixed configuration of the random-impurity distribution. In the next two sections we will apply the Matsubara-Toyozawa configuration-average scheme⁵ to the Green's-function matrices in order to calculate the impurity-band density of states and the impurity conductivity.

IV. IMPURITY BAND

The ensemble-average method of Matsubara-Toyozawa assumes a complete random nature of the spatial impurity distribution and allows the positions of all intermediate impurity sites $\{k_i\}$ in Eqs. (25) and (26) run over the whole space with equal probability. In principle, one can also introduce a pair-correlation function Λ_{ij} between the (i,j) -pair impurities. We may replace the summation over intermediate impurity sites by integral $\sum_i \rightarrow N \int d\mathbf{R}_i$, and define a sum of all possible journeys starting from the i th impurity and ending at the same i th impurity:

$$\begin{aligned} \underline{\eta}^\sigma(E) &= \underline{g}(E) \mathcal{P} \int \underline{T}_{i1} \underline{N} \underline{G}_0^\sigma(E) \underline{T}_{1i} \Lambda_{i1} d\mathbf{R}_1 + \underline{g}(E) \mathcal{P} \int \underline{T}_{i1} \underline{N} \underline{G}_0^\sigma(E) \underline{T}_{12} \underline{N} \underline{G}_0^\sigma(E) \underline{T}_{2i} \Lambda_{i1} \Lambda_{12} \Lambda_{2i} d\mathbf{R}_1 d\mathbf{R}_2 \\ &+ \underline{g}(E) \mathcal{P} \int \underline{T}_{i1} \underline{N} \underline{G}_0^\sigma(E) \underline{T}_{12} \underline{N} \underline{G}_0^\sigma(E) \underline{T}_{23} \underline{N} \underline{G}_0^\sigma(E) \underline{T}_{3i} \Lambda_{i1} \Lambda_{12} \Lambda_{23} \Lambda_{3i} d\mathbf{R}_1 d\mathbf{R}_2 d\mathbf{R}_3 + \dots \end{aligned} \quad (27)$$

It is impossible to calculate $\underline{\eta}^\sigma(E)$ if all possible journeys are considered. Matsubara and Toyozawa have argued that the most important contribution to $\underline{\eta}^\sigma(E)$ is from all *irreducible* journeys which never pass the origin site on the way.⁵ Although this Matsubara-Toyozawa *Ansatz* has not been justified rigorously, it has been commonly accepted by almost every author to study the electron-correlation effect in disordered systems. Later when we compare our result to that derived from the computer simulation, the agreement can be considered as a strong suggestion that the Matsubara-Toyozawa ensemble-average scheme is satisfactory.

Since the way to select irreducible journeys has been described in details in the original paper of Matsubara and Toyozawa,⁵ here we will present only the final result. The configurationally averaged diagonal (in terms of the impurity positions) Green's-function matrix $\langle \underline{G}^\sigma(i,i;E) \rangle_c$ can be expressed as

$$\begin{aligned} \underline{\xi}^\sigma(E) &\equiv \langle \underline{G}^\sigma(i,i;E) \rangle_c = \sum_{m=0}^{\infty} [\underline{\eta}^\sigma(E)]^m \underline{G}_0^\sigma(E) \\ &= [\underline{I} - \underline{\eta}^\sigma(E)]^{-1} \underline{G}_0^\sigma(E). \end{aligned} \quad (28)$$

To dress the vertices, all the \underline{G}_0^σ in Eq. (27) should be replaced by $\underline{\xi}^\sigma(E)$. Within the Matsubara-Toyozawa scheme, it is easier to calculate $\underline{\eta}^\sigma(E)$ in the reciprocal space. Let us define the Fourier transforms

$$\underline{\varepsilon}(\mathbf{k}) = \int \underline{T}_{j0} \Lambda_{j0} \exp(-i\mathbf{k} \cdot \mathbf{R}_j) d\mathbf{R}_j, \quad (29)$$

$$\underline{\varepsilon}_0(\mathbf{k}) = \int \underline{T}_{j0} \exp(-\mathbf{k} \cdot \mathbf{R}_j) d\mathbf{R}_j. \quad (30)$$

Then, Eq. (27) can be simply expressed as

$$\begin{aligned} \underline{\eta}^\sigma(E) &= \left[\frac{1}{2\pi} \right]^{-3} \underline{g}(E) \mathcal{P} \int \underline{\varepsilon}(\mathbf{k}) \underline{N} \underline{\xi}^\sigma(E) \\ &\quad \times \{ \underline{\varepsilon}(\mathbf{k}) [\underline{I} - \underline{N} \underline{\xi}^\sigma(E) \underline{\varepsilon}(\mathbf{k})]^{-1} \\ &\quad + \underline{\varepsilon}_0(\mathbf{k}) - \underline{\varepsilon}(\mathbf{k}) \} d\mathbf{k}. \end{aligned} \quad (31)$$

The two matrix equations (28) and (31) should be solved self-consistently. We notice from Eq. (21) that $\underline{G}_0^\sigma(E)$ is diagonal. Because of the projection operator \mathcal{P} , $\underline{\eta}^\sigma(E)$ is also diagonal. Therefore, from Eq. (28) it is obvious that $\underline{\xi}^\sigma(E)$ is diagonal.

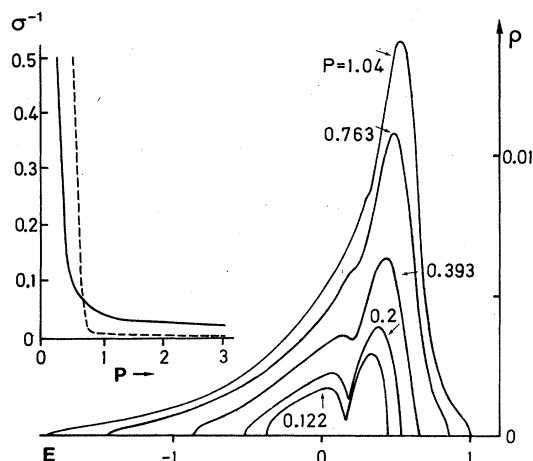


FIG. 1. Right part is the density of states for various impurity concentrations P , and the left part is the resistivity of Si:P (theory, solid curve; experiment, dashed curve).

The density of states of the impurity band is defined as

$$\begin{aligned}
 \rho^\sigma(E) &= -\frac{N}{\pi} \text{Im} \langle \langle a_{i\sigma}; a_{i\sigma}^\dagger \rangle \rangle_E \rangle_c \\
 &= -\frac{N}{\pi} \text{Im} \langle \langle b_{i\sigma} + c_{i\sigma}; b_{i\sigma}^\dagger + c_{i\sigma}^\dagger \rangle \rangle_E \rangle_c \\
 &= -\frac{N}{\pi} \text{Im} [\langle G_{bb}^\sigma(i, i; E) \rangle_c + \langle G_{cc}^\sigma(i, i; E) \rangle_c] \\
 &= -\frac{N}{\pi} \text{Im} [\text{Tr} \underline{\xi}^\sigma(E)]. \quad (32)
 \end{aligned}$$

It is important to point out that the above expression is a consequence of the static approximation, since in this case we have shown $\langle G_{bc}^\sigma(i, i; E) \rangle_c = 0$ and $\langle G_{cb}^\sigma(i, i; E) \rangle_c = 0$, i.e., $\underline{\xi}^\sigma(E)$ is diagonal. The density of states is so normalized such that the Fermi energy is determined from

$$\int_{-\infty}^{E_F} [\rho^+(E) + \rho^-(E)] dE = N, \quad (33)$$

where N is the impurity concentration.

Since there is no magnetic ordering observed in doped semiconductors, we will consider here only the nonmagnetic case for which $\rho^+(E) = \rho^-(E)$. A dimensionless impurity concentration $P = 32\pi N/a_0^3$, where a_0 is the effective Bohr radius, was first introduced by Matsubara and Toyozawa,⁵ and has been very popular for its convenience because for most doped semiconductors the critical concentration for the metal-insulator transition is around $P=1$ (more precisely around $P=0.8$). Using the matrix elements $t(\nu)_{ij}$ given by Eqs. (7)–(9), and assuming a constant value of $\Lambda_{ij}=1$, we have computed the impurity-band density of states. The results are shown in Fig. 1 for various values of impurity concentrations $P=0.122, 0.2, 0.393, 0.763$, and 1.04 . The zero reference energy has been shifted such that $E=0$ coincides with the ground-state energy of an isolated neutral impurity (D^0). Hence,

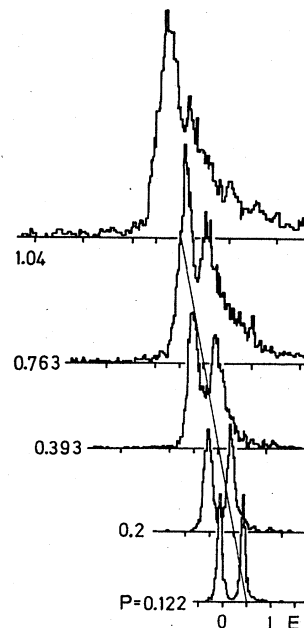


FIG. 2. Density of states derived from the computer simulation (Ref. 27).

the ground-state energy of an isolated negatively charged impurity (D^-) is 0.4741 . The bottom of the host conduction band lies at $E=0.5$. With decreasing impurity concentration, the formation of two split impurity subbands is clearly seen. Furthermore, when the impurity concentration approaches zero, the two subbands converge to two impurity levels exactly equal to the ground-state energies of D^0 and D^- , respectively.

Using the same impurity orbitals for D^0 and D^- as those defined in Sec. II, Riklund and Chao²⁷ have performed a computer simulation to obtain the impurity density of states. In the computer simulation a single Slater determinant modified with the Chandrasekhar D^- wave function has been incorporated to an improved unrestricted Hartree-Fock calculation. The nonorthogonality between impurity orbitals localized on different impurities was explicitly taken into account in the computer simulation. Furthermore, the computer simulation has retained all the matrix elements. The so-obtained density of states is shown in Fig. 2 for the impurity concentrations marked by the numbers. The long tail of the density of states at the low-energy side is due to small isolated impurity clusters. The characteristic features of such small isolated impurity clusters are averaged out in the Matsubara-Toyozawa scheme. Comparing the corresponding density of states curves in Figs. 1 and Fig. 2, we see that they form mirror images of each other, provided we neglect the low-energy tail in Fig. 2. In Sec. VI we will discuss the origin of this discrepancy.

V. IMPURITY CONDUCTIVITY

To calculate the conductivity, we need the Fourier transform of the Green's-function matrices. Starting from Eq. (26), we take the Matsubara-Toyozawa configuration average and then dress the vertices to obtain

$$\begin{aligned} \langle \underline{G}^\sigma(i, j; E) \rangle_c &= \underline{\xi}^\sigma(E) \underline{T}_{ij} \Lambda_{ij} \underline{\xi}^\sigma(E) + \underline{\xi}^\sigma(E) \int \underline{T}_{i_1} N \underline{\xi}^\sigma(E) \underline{T}_{i_1 j} \Lambda_{i_1} \Lambda_{i_1 j} d\mathbf{R}_1 \underline{\xi}^\sigma(E) \\ &+ \underline{\xi}^\sigma(E) \int \underline{T}_{i_1} N \underline{\xi}^\sigma(E) \underline{T}_{i_2} N \underline{\xi}^\sigma(E) \underline{T}_{i_2 j} \Lambda_{i_1} \Lambda_{i_2} \Lambda_{i_2 j} d\mathbf{R}_1 d\mathbf{R}_2 \underline{\xi}^\sigma(E) + \dots \end{aligned} \quad (34)$$

Taking the Fourier transform and making use of Eqs. (29) and (30), we have

$$\begin{aligned} \langle \underline{G}^\sigma(\mathbf{k}; E) \rangle_c &= \int \langle \underline{G}^\sigma(0, j; E) \rangle_c \exp(-i\mathbf{k} \cdot \mathbf{R}_j) d\mathbf{R}_j \\ &= \underline{\xi}^\sigma(E) \underline{\varepsilon}(\mathbf{k}) [\underline{I} - N \underline{\xi}^\sigma(E) \underline{\varepsilon}(\mathbf{k})]^{-1} \underline{\xi}^\sigma(E). \end{aligned} \quad (35)$$

According to Kubo,³² the static conductivity is given by

$$\underline{\Sigma}(0) = \lim_{\Omega \rightarrow 0^+} \underline{\Sigma}(\Omega), \quad (36)$$

where

$$\underline{\Sigma}(\Omega) = \int_0^\infty \exp[(i\Omega - \eta)t] dt \int_0^\beta \langle \mathbf{J}(0) \mathbf{J}(t + i\hbar\lambda) \rangle d\lambda \quad (37)$$

with $\beta = 1/k_B T$ and $\eta \rightarrow 0^+$. If we define

$$J_{\mu\nu}(\omega) = \int_{-\infty}^\infty \langle J_\mu(0) J_\nu(t) \rangle \exp(i\omega t) dt, \quad (38)$$

then, the $\mu\nu$ component of $\underline{\Sigma}(\Omega)$ can be simplified to

$$\Sigma_{\mu\nu}(\Omega) = -\frac{1}{2\hbar\Omega} (e^{\beta\hbar\Omega} - 1) J_{\mu\nu}(\Omega). \quad (39)$$

The fluctuation-dissipation theorem yields the relation

$$(e^{\beta\hbar\Omega} - 1) J_{\mu\nu}(\Omega) = - \int_{-\infty}^\infty \langle [J_\mu(0), J_\nu(\tau)]_- \rangle e^{i\omega\tau} d\tau. \quad (40)$$

$$\begin{aligned} \langle [J_\mu(0), J_\nu(\tau)]_- \rangle &= -(e^2/\hbar^2) \sum_{i,j,\sigma,p,q,s} \mathbf{R}_{i,j,\mu} \mathbf{R}_{pq,\nu} \mathcal{S} \begin{bmatrix} t(1)_{ij} & t(2)_{ij} \\ t(2)_{ij} & t(3)_{ij} \end{bmatrix} \begin{bmatrix} \langle [b_{i\sigma}^\dagger(0) b_{j\sigma}(0) \rangle \langle [b_{i\sigma}^\dagger(0) c_{j\sigma}(0) \rangle \\ \langle [c_{i\sigma}^\dagger(0) b_{j\sigma}(0) \rangle \langle [c_{i\sigma}^\dagger(0) c_{j\sigma}(0) \rangle \end{bmatrix} \\ &\times \begin{bmatrix} t(1)_{pq} & t(2)_{pq} \\ t(2)_{pq} & t(3)_{pq} \end{bmatrix} \begin{bmatrix} b_{ps}(\tau) b_{qs}(\tau) \rangle_- & b_{ps}(\tau) c_{qs}(\tau) \rangle_- \\ c_{ps}(\tau) b_{qs}(\tau) \rangle_- & c_{ps}(\tau) c_{qs}(\tau) \rangle_- \end{bmatrix}. \end{aligned} \quad (44)$$

For given cluster of impurities (i, j, p, q) and given spin arrangement (σ, s) , there are 16 correlation functions of the form $\langle [A_{i\sigma}^\dagger(0) B_{j\sigma}(0), C_{ps}^\dagger(\tau) D_{qs}(\tau)]_- \rangle$ appearing on the right-hand side of Eq. (44). The application of the static approximation slightly simplifies the problem by imposing a restriction $s = \sigma$. Using the fluctuation-dissipation theorem, all these correlation functions can be expressed in terms of the Green's-function matrices. We will not show the explicit mathematical manipulation which is very long but straightforward. The final result is

$$\begin{aligned} \Sigma_{\mu\nu}(0) &= -(e^2/\pi\hbar) \sum_{\sigma} \sum_{i,j,p,q} \mathbf{R}_{ij,\mu} \mathbf{R}_{pq,\nu} \int_{-\infty}^\infty dE \left[-\frac{\partial f(E)}{\partial E} \right] \mathcal{S} \begin{bmatrix} t(1)_{ij} & t(2)_{ij} \\ t(2)_{ij} & t(3)_{ij} \end{bmatrix} \begin{bmatrix} \text{Im} G_{bb}^\sigma(j, p; E) & \text{Im} G_{bc}^\sigma(j, p; E) \\ \text{Im} G_{cb}^\sigma(j, p; E) & \text{Im} G_{cc}^\sigma(j, p; E) \end{bmatrix} \\ &\times \begin{bmatrix} t(1)_{pq} & t(2)_{pq} \\ t(2)_{pq} & t(3)_{pq} \end{bmatrix} \begin{bmatrix} \text{Im} G_{bb}^\sigma(q, i; E) & \text{Im} G_{bc}^\sigma(q, i; E) \\ \text{Im} G_{cb}^\sigma(q, i; E) & \text{Im} G_{cc}^\sigma(q, i; E) \end{bmatrix}. \end{aligned} \quad (45)$$

Since the distribution of the impurities is random, the conductivity must be isotropic and so the conductivity tensor $\underline{\Sigma}(0)$ is diagonal $\underline{\Sigma}(0) \underline{I}$ with

$$\Sigma(0) = -(e^2/3\pi\hbar) \sum_{\sigma} \int_{-\infty}^\infty dE \left[-\frac{\partial f(E)}{\partial E} \right] \Xi^\sigma(E), \quad (46)$$

where

$$\Xi^\sigma(E) = \sum_{ijpq} \mathcal{S} \mathbf{R}_{ij} \begin{bmatrix} t(1)_{ij} & t(2)_{ij} \\ t(2)_{ij} & t(3)_{ij} \end{bmatrix} \begin{bmatrix} \text{Im} G_{bb}^\sigma(j, p; E) & \text{Im} G_{bc}^\sigma(j, p; E) \\ \text{Im} G_{cb}^\sigma(j, p; E) & \text{Im} G_{cc}^\sigma(j, p; E) \end{bmatrix} \times \mathbf{R}_{pq} \begin{bmatrix} t(1)_{pq} & t(2)_{pq} \\ t(2)_{pq} & t(3)_{pq} \end{bmatrix} \begin{bmatrix} \text{Im} G_{bb}^\sigma(q, i; E) & \text{Im} G_{bc}^\sigma(q, i; E) \\ \text{Im} G_{cb}^\sigma(q, i; E) & \text{Im} G_{cc}^\sigma(q, i; E) \end{bmatrix}. \quad (47)$$

The commutator is readily derived from the current operator

$$\mathbf{J} = \frac{ie}{\hbar} \left[H, \sum_{i,\sigma} \mathbf{R}_i a_{i\sigma}^\dagger a_{i\sigma} \right]_- = \frac{ie}{\hbar} \sum_{i,\sigma} \mathbf{R}_i [H, b_{i\sigma}^\dagger b_{i\sigma} + c_{i\sigma}^\dagger c_{i\sigma}]_-. \quad (41)$$

To put the final result in a compact form, we adopt the notations

$$\mathcal{S} \begin{bmatrix} A & B \\ C & D \end{bmatrix} = A + B + C + D, \quad (42)$$

$$\begin{aligned} &\begin{bmatrix} \langle [A \langle [B \begin{bmatrix} a \rangle_- \ b \rangle_- \rangle \\ \langle [C \langle [D \begin{bmatrix} c \rangle_- \ d \rangle_- \rangle \end{bmatrix} \end{bmatrix} \\ &= \begin{bmatrix} \langle [A, a]_- + [B, c]_- \rangle \langle [A, b]_- + [B, d]_- \rangle \\ \langle [C, a]_- + [D, c]_- \rangle \langle [C, b]_- + [D, d]_- \rangle \end{bmatrix}, \end{aligned} \quad (43)$$

and $\mathbf{R}_{ij} = \mathbf{R}_i - \mathbf{R}_j$. A tedious algebraic manipulation then leads to

In the above equations, $f(E)$ is the Fermi-Dirac distribution function.

The above derived conductivity is for a fixed impurity distribution. The next step is to take the configuration average over all possible random distributions of impurities. We have to perform 16 ensemble averages of the form $\langle G_{\mu\nu}^{\sigma}(j,p;E)G_{\kappa\lambda}^{\sigma}(q,i;E) \rangle_c$. Again we will follow the argument of Matsubara-Toyozawa⁵ to approximate

$$\langle G_{\mu\nu}^{\sigma}(j,p;E)G_{\kappa\lambda}^{\sigma}(q,i;E) \rangle_c \simeq \langle G_{\mu\nu}^{\sigma}(j,p;E) \rangle_c \langle G_{\kappa\lambda}^{\sigma}(q,i;E) \rangle_c. \quad (48)$$

After one more lengthy calculation which is too long to be shown here, a compact form of the dc impurity conductivity is derived as

$$\Sigma(0) = -(e^2/3\pi\hbar) \sum_{\sigma} \int_{-\infty}^{\infty} dE \left[-\frac{\partial f(E)}{\partial E} \right] [\Xi_1^{\sigma}(E) + \Xi_2^{\sigma}(E)], \quad (49)$$

where

$$\begin{aligned} \Xi_1^{\sigma}(E) &= \mathcal{L}(-1/8\pi^3) \int \{ \nabla_{\mathbf{k}} \underline{\epsilon}(\mathbf{k}) [N \text{Im} \underline{\xi}^{\sigma}(E) + N^2 \text{Im} \langle \underline{G}^{\sigma}(\mathbf{k};E) \rangle_c] \}^2 d\mathbf{k} \\ &+ \mathcal{L}(-1/8\pi^3) \int \nabla_{\mathbf{k}} \underline{\epsilon}(\mathbf{k}) N \text{Im} \underline{\xi}^{\sigma}(E) \cdot \nabla_{\mathbf{k}} [\underline{\epsilon}_0(\mathbf{k}) - \underline{\epsilon}(\mathbf{k})] N \text{Im} \underline{\xi}^{\sigma}(E) d\mathbf{k} \end{aligned} \quad (50)$$

and

$$\begin{aligned} \Xi_2^{\sigma}(E) &= \mathcal{L} \int \mathbf{R}_j T_{0j} \Lambda_{0j} \left[\left[\frac{1}{2\pi} \right]^3 N \int \text{Im} \langle \underline{G}^{\sigma}(\mathbf{k};E) \rangle_c \exp(i\mathbf{k} \cdot \mathbf{R}_j) d\mathbf{k} \right] \\ &\cdot \mathbf{R}_j T_{j0} \left[\left[\frac{1}{2\pi} \right]^3 N \int \text{Im} \langle \underline{G}^{\sigma}(\mathbf{k};E) \rangle_c \exp(i\mathbf{k} \cdot \mathbf{R}_j) d\mathbf{k} \right] d\mathbf{R}_j. \end{aligned} \quad (51)$$

Numerical calculation indicates that $\Xi_2^{\sigma}(E)$ is negligibly small as compared to $\Xi_1^{\sigma}(E)$. The same conclusion was obtained by Matsubara and Toyozawa⁵ in their single-impurity-band model calculation for randomly distributed impurities without correlation. In our calculation again we have set $\Lambda_{ij} = 1$ in order to avoid the unnecessary complication in numerical computation. We have applied our analysis of dc conductivity to the phosphorus-doped silicon. From the measured ionization energy of an isolated neutral impurity, the effective Bohr radius is determined as 13.2 Å. Our calculated resistivity is shown in Fig. 1 (solid curve) as a function of the impurity concentration P . The measured resistivity³³ is also plotted as dashed curve for comparison. Since in the next section we will discuss the possible improvement of the present calculation, we will not make further comment on the agreement between the theory and the experiment.

VI. DISCUSSION

Our split-impurity-subband Hamiltonian Eq. (5) is a simplified version of the complete Hamiltonian based on which the computer simulation^{27,28} was performed. This simpler Hamiltonian still retains the most important electron-correlation effect, namely, the matrix elements depend crucially on the local electron distribution. In our analysis we have assumed the anticommutation relation for the operators $\{a_{i\sigma}^{\dagger}, a_{i\sigma}\}$. This is equivalent to the assumption that impurity orbitals localized on different neutral impurities are orthogonal. However, in the computer simulation the overlap between different impurity orbitals has been explicitly taken into account. The nonorthogonality effect has been studied analytically using an uncorrelated single-impurity-band model.³⁴⁻³⁶ The result of Yonezawa *et al.* (Figs. 1 and 2 of Ref. 35) is reproduced in Fig. 3 as parts (c) and (d). If we assume the

orthogonality, the density of states is given as part (c) for various impurity concentrations. When the nonorthogonality correction is introduced, the curves of part (c) change into the corresponding curves in part (d), as if following a mirror-image transformation. Computer simulations based on various single-impurity-band models are also available.^{37,38} Parts (a) and (b) in Fig. 3 are reproduced from Ref. 38. Again, the density-of-states curves derived with [part (b)] and without [part (a)] the assumption of orthogonality form a pair of mirror images. Therefore, we come to the conclusion that the discrepancy between the density-of-states curves shown in Figs. 1 and 2 has its origin in the orthogonality assumption. If we include the nonorthogonality correction to improve our analysis, it is reasonable to believe that the so-obtained results should agree very well with those derived from the computer simulation. If we accept this conclusion, it is also reasonable to believe that the static approximation and the Matsubara-Toyozawa configuration average

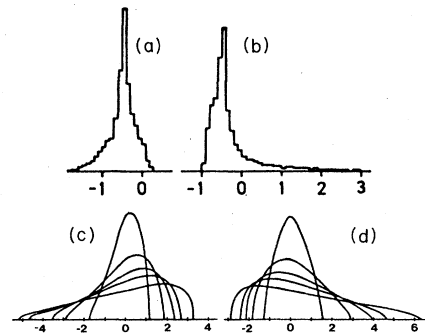


FIG. 3. Density of states obtained with different approximations and using different models. See the text for details.

scheme do not cause large error.

In the Introduction we have emphasized the role of the host conduction band for a complete study of the metal-insulator transition in doped semiconductors. In our paper the host conduction band has been ignored. From Eq. (33) we have calculated the Fermi energy for various impurity concentrations: $(P; E_F) = (0.122; 0.15)$, $(0.2; 0.17)$, $(0.393; 0.20)$, $(0.763; 0.25)$, and $(1.04; 0.28)$. Let us remind ourselves that the bottom of the host conduction band (assumed not changed even when doped) lies at $E_b = 0.5$. The unreasonably large separation $E_b - E_F$ for the impurity concentration $N > 0.393$ strongly suggests the necessity of a three-band model: two split impurity subbands plus the host conduction band. When electrons occupy

the conduction-band states, they can efficiently screen the impurity potential. The net effect will be a downward shift of the conduction-band edge and an upward shift of the donor impurity band.

To close this paper, we should mention that if we set $E_1 = \epsilon_2$ and $t(1)_{ij} = t(2)_{ij} = t(3)_{ij}$, our analysis reduces to exactly that of Matsubara and Toyozawa.⁵

ACKNOWLEDGMENTS

This work is financially supported by the Swedish Natural Science Research Council under Grant No. NFR FFU 3996-121.

*Permanent address: Department of Physics, Tsinghua University, Beijing, People's Republic of China.

¹For a recent review, see *Electron-Electron Interaction in Disordered Systems*, edited by M. Pollak and A. L. Efros (North-Holland, Amsterdam, in press).

²J. Serre and A. Ghazali, *Phys. Rev. B* **28**, 4704 (1983).

³M. S. Figueira, S. S. Makler, and E. V. Anda, *J. Phys. C* **17**, 623 (1984).

⁴J. Hubbard, *Proc. R. Soc. London, Ser. A* **276**, 238 (1963); **281**, 401 (1964).

⁵T. Matsubara and Y. Toyozawa, *Prog. Theor. Phys.* **26**, 739 (1961).

⁶M. Kikuchi, *J. Phys. Soc. Jpn.* **25**, 989 (1968).

⁷A. Aoki and H. Kamimura, *J. Phys. Soc. Jpn.* **40**, 6 (1976).

⁸H. Nishimura, *Phys. Rev.* **138**, A815 (1965).

⁹A. Ferreira da Silva, R. Kishore, and I. C. da Cunha Lima, *Phys. Rev. B* **23**, 4035 (1981).

¹⁰M. Taniguchi, M. Hirano, and S. Narita, *Phys. Rev. Lett.* **35**, 1095 (1975).

¹¹P. Norton, *Phys. Rev. Lett.* **37**, 164 (1976).

¹²M. Taniguchi and S. Narita, *Solid State Commun.* **20**, 131 (1976).

¹³M. Taniguchi and S. Narita, *J. Phys. Soc. Jpn.* **43**, 1262 (1977).

¹⁴T. Kawabata, M. Muro, and S. Narita, *Solid State Commun.* **23**, 267 (1977).

¹⁵M. Taniguchi, S. Narita, N. Hasegawa, and M. Kobayashi, *J. Phys. Soc. Jpn.* **45**, 545 (1978).

¹⁶M. Taniguchi and S. Narita, *J. Phys. Soc. Jpn.* **47**, 1503 (1979).

¹⁷M. Kobayashi, S. Sawada, and S. Narita, *J. Phys. Soc. Jpn.* **51**, 844 (1982).

¹⁸S. Narita, T. Shinbashi, and M. Kobayashi, *J. Phys. Soc. Jpn.* **51**, 2186 (1982).

¹⁹M. Capizzi, G. A. Thomas, F. DeRosa, R. N. Bhatt, and R. M. Rice, *Solid State Commun.* **31**, 611 (1979).

²⁰G. A. Thomas, M. Gapizzi, F. DeRosa, R. N. Bhatt, and T. M. Rice, *Phys. Rev. B* **23**, 5472 (1981).

²¹A. Natori and H. Kamimura, *J. Phys. Soc. Jpn.* **44**, 1216 (1978).

²²A. Natori and H. Kamimura, *J. Phys. Soc. Jpn.* **47**, 1550 (1979).

²³R. N. Bhatt and T. M. Rice, *Phys. Rev. B* **23**, 1920 (1981).

²⁴J. Golka, *Philos. Mag.* **B 40**, 513 (1979).

²⁵A. Ghazali and P. Leroux-Hugon, *Phys. Rev. Lett.* **41**, 1569 (1978).

²⁶S. Chandrasekhar, *Astrophys. J.* **100**, 176 (1944).

²⁷R. Riklund and K. A. Chao, *Phys. Rev. B* **26**, 2168 (1982).

²⁸R. Riklund and K. A. Chao, *Phys. Rev. B* **29**, 3456 (1984).

²⁹Y. Wu and L. M. Falicov, *Phys. Rev. B* **29**, 3671 (1984).

³⁰P. Petelenz and V. H. Smith, Jr., *Phys. Rev. B* **21**, 4884 (1980).

³¹C. L. Pekeris, *Phys. Rev.* **126**, 1470 (1962).

³²R. Kubo, *J. Phys. Soc. Jpn.* **12**, 570 (1957).

³³C. Yamanouchi, K. Mizuguchi, and W. Sasaki, *J. Phys. Soc. Jpn.* **22**, 859 (1967).

³⁴Y. Ishida and F. Yonezawa, *Prog. Theor. Phys.* **49**, 731 (1973).

³⁵F. Yonezawa, Y. Ishida, and F. Martino, *J. Phys. F* **6**, 1091 (1976).

³⁶N. Majlis and E. Anda, *J. Phys. C* **11**, 1607 (1978).

³⁷M. Weissmann and N. V. Cohan, *J. Phys. F* **7**, 913 (1977).

³⁸K. A. Chao, A. Ferreira da Silva, and R. Riklund, *Prog. Theor. Phys. Suppl. No.* **72**, 181 (1982).